

REPORT DOCUMENTATION PAGE

Form Approved
OMB No. 0704-0188

Public reporting burden for this collection of information is estimated to average 1 hour per response, including the time for reviewing instructions, searching existing data sources, gathering and maintaining the data needed, and completing and reviewing this collection of information. Send comments regarding this burden estimate or any other aspect of this collection of information, including suggestions for reducing this burden to Department of Defense, Washington Headquarters Services, Directorate for Information Operations and Reports (0704-0188), 1215 Jefferson Davis Highway, Suite 1204, Arlington, VA 22202-4302. Respondents should be aware that notwithstanding any other provision of law, no person shall be subject to any penalty for failing to comply with a collection of information if it does not display a currently valid OMB control number. **PLEASE DO NOT RETURN YOUR FORM TO THE ABOVE ADDRESS.**

1. REPORT DATE (DD-MM-YYYY) 16-02-2006		2. REPORT TYPE Journal Article		3. DATES COVERED (From - To)	
4. TITLE AND SUBTITLE The Convergence of CASSCF-CISD Energies to the Complete Basis Set Limit (PREPRINT)				5a. CONTRACT NUMBER F04611-03-C-0015	
				5b. GRANT NUMBER	
				5c. PROGRAM ELEMENT NUMBER	
6. AUTHOR(S) George Petersson & David Malick (Wesleyan Univ.); Michael Frisch (Gaussian, Inc.); Matthew Braunstein (Spectral Sciences, Inc.)				5d. PROJECT NUMBER BMSBR2FT	
				5e. TASK NUMBER	
				5f. WORK UNIT NUMBER	
7. PERFORMING ORGANIZATION NAME(S) AND ADDRESS(ES) Spectral Sciences Incorporated 4 Fourth Avenue Burlington MA 01803-3304				8. PERFORMING ORGANIZATION REPORT NUMBER AFRL-PR-ED-JA-2006-037	
9. SPONSORING / MONITORING AGENCY NAME(S) AND ADDRESS(ES) Air Force Research Laboratory (AFMC) AFRL/PRS 5 Pollux Drive Edwards AFB CA 93524-70448				10. SPONSOR/MONITOR'S ACRONYM(S)	
				11. SPONSOR/MONITOR'S NUMBER(S) AFRL-PR-ED-JA-2006-037	
12. DISTRIBUTION / AVAILABILITY STATEMENT Approved for public release; distribution unlimited (PA no. AFRL-ERS-PAS-2006-034)					
13. SUPPLEMENTARY NOTES Submitted for publication in Journal of Chemical Physics					
14. ABSTRACT Examination of the convergence of full valence CASSCF-CISD energies with expansion of the one-electron basis set reveals a pattern very similar to the convergence of single determinant CCSD energies. Calculations on the lowest four singlet states and the lowest four triplet states of N ₂ with the sequence of ntuple- \square augmented polarized (nZaP) basis sets (n = 2, 3, 4, 5, and 6) are used to establish the complete basis set (CBS) limits. Full CI and core electron contributions must be included for very accurate potential energy surfaces. However, a simple extrapolation scheme that has no adjustable parameters and requires nothing more demanding than CAS(10e-8orb)-CISD/3ZaP calculations gives the R _e , \square_e , $\square_e X_e$, T _e and D _e for these eight states with rms errors of 0.0006 Å, 4.43 cm ⁻¹ , 0.35 cm ⁻¹ , 0.063 eV, and 0.018 eV respectively.					
15. SUBJECT TERMS					
16. SECURITY CLASSIFICATION OF:			17. LIMITATION OF ABSTRACT	18. NUMBER OF PAGES	19a. NAME OF RESPONSIBLE PERSON
a. REPORT	b. ABSTRACT	c. THIS PAGE			Dr. Marty J. Venner
Unclassified	Unclassified	Unclassified	A	30	19b. TELEPHONE NUMBER (include area code) N/A

The convergence of CASSCF-CISD energies to the complete basis set limit (Preprint).

George A. Petersson and David K Malick, *Hall-Atwater Laboratories of Chemistry, Wesleyan University, Middletown, Connecticut 06459-0180*

Michael J. Frisch, *Gaussian, Inc., 340 Quinnipiac St. Bldg. 40, Wallingford, Connecticut 06492-4050*

Matthew Braunstein, *Spectral Sciences, Inc., 4 Fourth Avenue, Burlington, Massachusetts 01803-3304*

(Received

Examination of the convergence of full valence CASSCF-CISD energies with expansion of the one-electron basis set reveals a pattern very similar to the convergence of single determinant CCSD energies. Calculations on the lowest four singlet states and the lowest four triplet states of N_2 with the sequence of n -tuple- ζ augmented polarized (nZaP) basis sets ($n = 2, 3, 4, 5,$ and 6) are used to establish the complete basis set (CBS) limits. Full CI and core electron contributions must be included for very accurate potential energy surfaces. However, a simple extrapolation scheme that has no adjustable parameters and requires nothing more demanding than CAS(10e-,8orb)-CISD/3ZaP calculations gives the R_e , ω_e , $\omega_e X_e$, T_e and D_e for these eight states with rms errors of 0.0006 Å, 4.43 cm^{-1} , 0.35 cm^{-1} , 0.063 eV, and 0.018 eV respectively.

I. INTRODUCTION

Virtually all *ab initio* electronic structure calculations employ expansions in basis sets of atomic orbitals. Modern treatments of electron correlation such as CCSD(T)^{1,2}, CASPT2³, and CAS-CISD^{4,7}, have reduced the errors from the many-body expansion to the point where truncation of this one-particle basis set is the dominant source of error in these calculations.⁸ Over the past twenty years, it has become evident that the slow convergence of molecular energies would require the use of prohibitively large atomic orbital basis sets to achieve “chemical accuracy” of ~ 1 kcal/mol directly. It is therefore necessary to either employ empirical corrections^{9,10}, or attempt to extrapolate to the complete basis set (CBS) limit.¹¹⁻¹⁴ Extrapolation schemes for calculations employing a single reference configuration are now used routinely¹¹⁻¹⁴. Our previous paper¹⁵ developed an extrapolation scheme for CASSCF calculations. In this paper we shall examine the convergence of the dynamic correlation component from multi-reference methods to the complete one-electron basis set (CBS) limit.

Many problems require higher accuracy than can be achieved with computationally accessible basis sets. For example, the reaction, $O(^3P) +$

$\text{HCl}(v=2, j=1, 6, 9) \rightarrow \text{OH}(v', j') + \text{Cl}(^2\text{P})$, exhibits large differences between measured $\text{OH}(v', j')$ distributions and benchmark quantum scattering calculations on recently computed multi-reference potential surfaces with large basis sets, suggesting a need for re-examination of the surfaces with higher accuracy.¹⁶ Another example is the reaction, $\text{O}(^3\text{P}) + \text{H}_2\text{O} \rightarrow \text{OH}(\text{A}) + \text{OH}(\text{X})$, observed in space-based¹⁷ and laboratory experiments.¹⁸ Recent work using multi-reference wave functions and large basis sets has mapped the conical intersection mechanism of this reaction.¹⁹ However, an explanation of the magnitude of the total cross section and product state distributions will require chemically accurate energies over large portions of the potential surfaces involved - a task that would be prohibitively expensive with basis sets that are sufficient to ensure chemical accuracy. Many other reactions of open-shell species with singlet molecules, such as $\text{O}(^3\text{P})$ reactions with hydrocarbons, are now being studied at hyperthermal energies,²⁰ and may require multi-reference wave functions where computation of chemically accurate energies using large basis sets would again be prohibitively expensive.

Our approach will be to systematically examine the convergence of the electronic energy with the one-electron basis set for each component of the energy. In a previous paper, we examined the convergence of the multi-reference CASSCF energy¹⁵. We found that a computationally inexpensive single reference UHF calculation with two different size basis sets provided a means of extrapolating the multi-reference CASSCF energy to the complete basis set limit. In the present paper, we will examine the convergence with the one-electron basis set of the dynamic correlation energy at several levels: MP2, CCSD, CCSD(T), and CAS-CISD. We find that single reference MP2 and CCSD calculations provide a model for the basis set convergence of the dynamic component of multi-reference CAS-CISD calculations. In this way, we develop an extrapolation formula that requires nothing more demanding than CAS(10e-, 8orb)-CISD calculations within a modest sized triple- ζ basis set.

We will examine the first 8 electronic states of N_2 , as a case study, since highly accurate theoretical and experimental data are available to test the new methods. It is important to note that convergence with basis set is studied with a sequence of n -tuple- ζ augmented polarized ($n\text{ZaP}$) basis sets ($n = 2, 3, 4, 5, \text{ and } 6$) which were developed by requiring uniform convergence of each component of both the SCF and the correlation energy.²¹⁻²³ Although we are primarily interested in the basis set convergence of valence electron CAS-CISD calculations, we shall also consider Full CI and core-valence corrections. This will provide a check on our extrapolation method through quantitative comparisons with experimental data.

II. EXCITED STATE MODELS

We shall develop a multi-reference model chemistry based on the full valence complete active space self consistent field (CASSCF) reference.²⁴⁻²⁸ These calculations employ a full CI within a variationally optimized set of molecular orbitals that is uniquely determined by the number of valence-shell orbitals of the constituent atoms. They are a size consistent MCSCF extension of single determinant Hartree-Fock theory and require no subjective choices. These CASSCF methods are thus an appropriate starting point for a model chemistry.²⁹⁻³¹

We have selected the lowest four singlet states and the lowest four triplet states of N_2 for this study, since there is a wealth of experimental and computational results available for comparison (Table I). We first examine the basis set convergence of single configuration UHF energies, since we have shown that they are useful models for the convergence of CASSCF energies.¹⁵ Note that we use the same UHF reference for Σ and Δ ($\pi \rightarrow \pi^*$) excited states, since our previous work demonstrated that the specific UHF state employed for comparison with CAS calculations was not important as long as the

Table I. The eight low-lying states of N_2 considered in this paper.

State	Configuration	R_{NN} (Å)		
		UHF/2ZaP	CAS(10e,8orb)/2ZaP	Experiment ^a
$X^1\Sigma_g^+$	$(1\sigma_g^2, 1\sigma_u^2, 2\sigma_g^2, 2\sigma_u^2, 3\sigma_g^2, 1\pi_u^4)$	1.0754	1.1148	1.0977
$A^3\Sigma_u^+$	$(1\sigma_g^2, 1\sigma_u^2, 2\sigma_g^2, 2\sigma_u^2, 3\sigma_g^2, 1\pi_u^3, 1\pi_g)$	1.2374 ^b	1.3069	1.2866
$B^3\Pi_g$	$(1\sigma_g^2, 1\sigma_u^2, 2\sigma_g^2, 2\sigma_u^2, 3\sigma_g, 1\pi_u^4, 1\pi_g)$	1.1918	1.2320	1.2126
$W^3\Delta_u$	$(1\sigma_g^2, 1\sigma_u^2, 2\sigma_g^2, 2\sigma_u^2, 3\sigma_g^2, 1\pi_u^3, 1\pi_g)$	1.2374 ^b	1.2980	1.2833 ^d
$B^3\Sigma_u^-$	$(1\sigma_g^2, 1\sigma_u^2, 2\sigma_g^2, 2\sigma_u^2, 3\sigma_g^2, 1\pi_u^3, 1\pi_g)$	1.2374 ^b	1.2984	1.2784
$a^1\Sigma_u^-$	$(1\sigma_g^2, 1\sigma_u^2, 2\sigma_g^2, 2\sigma_u^2, 3\sigma_g^2, 1\pi_u^3, 1\pi_g)$	1.2383 ^c	1.2927	1.2755
$a^1\Pi_g$	$(1\sigma_g^2, 1\sigma_u^2, 2\sigma_g^2, 2\sigma_u^2, 3\sigma_g, 1\pi_u^4, 1\pi_g)$	1.2017	1.2395	1.2203
$w^1\Delta_u$	$(1\sigma_g^2, 1\sigma_u^2, 2\sigma_g^2, 2\sigma_u^2, 3\sigma_g^2, 1\pi_u^3, 1\pi_g)$	1.2383 ^c	1.2865	1.268

a. Reference 32.

b. & c. These UHF wavefunctions are mixtures of Σ and Δ states.

d. No experimental value was available. This is the CAS-CISD/5ZaP calculated geometry.

UHF calculations used the same geometry and occupied the same orbitals as the CAS calculation.¹⁵ We also examine the basis set convergence of single reference MP2 and CCSD(T) energies to provide models for the convergence of CAS-CISD energies. Full configuration interaction (FCI) energies and core electron correlation energies are included in order to make comparisons with experiment.

We shall now examine the basis set convergence of UHF, UMP2, UCCSD(T), CAS(10e-,8orb), CAS-CISD, and FCI calculations at the experimental geometries in Table I. Most numerical results in this paper were obtained with a modified version of the Gaussian suite of programs.³³ However, the CAS-CISD calculations employed the Columbus programs.³⁴⁻³⁷

III. CONVERGENCE OF THE ENERGY TO THE CBS LIMIT

Extrapolation requires a well defined sequence of approximations and a model for the convergence of this sequence. The expansion of molecular orbitals in increasing numbers of Gaussian basis functions provides a systematic sequence of approximations. Each component of the molecular electronic energy has its own distinct pattern of convergence. We must therefore develop a set of models, one for the convergence of each of the components of the molecular energy.

A. The SCF energy

The approximate exponential convergence of SCF energies with the number of Gaussian basis functions is well known.³⁸ As suggested by Kutzelnigg,^{39,40} the basis set truncation errors for these SCF calculations are actually better described by a function of the form:

$$\text{Error} \cong A \exp \left[-a \cdot n_p^{1/2} \right], \quad (1)$$

where n_p is the number of primitives and a is a parameter (Fig. 1). If we calculate the SCF energy with two different size basis sets comprised of n_1 and n_2 sets of optimized Gaussian basis functions respectively (with $n_2 > n_1$), then Eq.(1) provides the model for a linear extrapolation to the SCF limit.^{15,21}

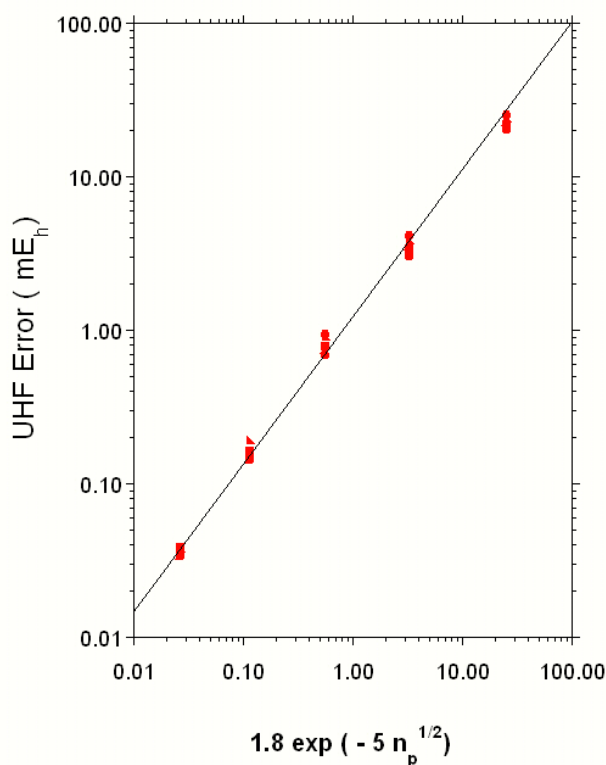


Fig. 1 The basis set convergence of the UHF energies of the N_2 states in Table I.

$$E_{SCF \text{ Limit}} \cong E(n_2) + \{\exp[a \cdot n_2^{1/2} - a \cdot n_1^{1/2}] - 1\}^{-1} \{E(n_2) - E(n_1)\}. \quad (2)$$

Note that the extrapolation does not explicitly include the coefficient, A in Eq.(1), which varies from one atom or molecule to another.

Extrapolations based on Eq.(2) require using a sequence of basis sets with *systematically* increasing numbers of Gaussian primitives for *each* angular momentum type combined with sets of polarization functions selected to give uniform convergence for each component of the molecular SCF energy. We have constructed such a balanced sequence of n -tuple- ζ augmented polarized (n ZaP) basis sets ($n = 2, 3, 4, 5,$ and 6) for which the parameter, a , is relatively constant, $a \sim 5$ (Fig. 1), for Hartree-Fock calculations at a fixed geometry.^{21,22} These basis sets include diffuse valence (i.e. s and p) functions permitting some mixing in of Rydberg states, but spare the cost of diffuse higher angular momentum functions. We note that throughout this paper we are using preliminary versions of these basis sets, which may differ from the final versions.²³ Substitution of $a=5$ and the appropriate values of n_1 and n_2 into Eq.(2):

$$E_{SCF \text{ Limit}} \cong E(6ZaP) + 0.309 \{E(6ZaP) - E(5ZaP)\}, \quad (3)$$

provides our best estimate of the HF limit. This extrapolation gives -108.9938169 hartree (E_h) for the SCF limit of the $X^1\Sigma_g^+$ ground state of N_2 at $R_{NN} = 2.068$ bohr, which is in good agreement with the numerical SCF energy at this geometry,⁴¹ $-108.9938256 E_h$. Since these n ZaP basis sets were optimized for atoms, it is reasonable to assume that the

Table II. The convergence of the UHF energies (hartree) to the CBS limit.

State	Basis Set					CBS[Eq.(3)]
	2ZaP	3ZaP	4ZaP	5ZaP	6ZaP	
$X^1\Sigma_g^+$	-108.967814	-108.988992	-108.992209	-108.993004	-108.993124	-108.993161
$A^3\Sigma_u^+$	-108.769142	-108.787873	-108.790430	-108.791051	-108.791176	-108.791215
$B^3\Pi_g$	-108.700891	-108.719275	-108.722135	-108.722733	-108.722846	-108.722881
$W^3\Delta_u$	-108.769573	-108.788325	-108.790888	-108.791513	-108.791638	-108.791676
$B^1\Sigma_u^-$	-108.770196	-108.788984	-108.791557	-108.792187	-108.792312	-108.792350
$a^1\Sigma_u^-$	-108.714405	-108.734254	-108.737143	-108.737848	-108.738001	-108.738048
$a^1\Pi_g$	-108.673750	-108.692598	-108.695347	-108.695946	-108.696054	-108.696088
$w^1\Delta_u$	-108.715139	-108.735050	-108.737954	-108.738667	-108.738819	-108.738866

UHF CBS energies of the valence excited states (Table II) are also accurate to about 10 microhartree (μE_h). We should also note that the extrapolations differ from the UHF/6ZaP energies by only 40 μE_h lending support to our 10 μE_h error estimate.

B. The CASSCF energy

The CASSCF wave function is similar to the SCF wave function in that it consists of a limited number of optimized self-consistent-field orbitals. We can therefore employ the UHF CBS limit obtained above to extrapolate our CAS calculations as described in our previous paper:¹⁵

$$E_{CAS}(CBS) \cong E_{CAS}(4ZaP) + [E_{UHF}(CBS) - E_{UHF}(4ZaP)] \left[\frac{E_{CAS}(4ZaP) - E_{CAS}(3ZaP)}{E_{UHF}(4ZaP) - E_{UHF}(3ZaP)} \right], \quad (4)$$

based on 3ZaP and 4ZaP calculations, or:

$$E_{CAS}(CBS) \cong E_{CAS}(5ZaP) + [E_{UHF}(CBS) - E_{UHF}(5ZaP)] \left[\frac{E_{CAS}(5ZaP) - E_{CAS}(4ZaP)}{E_{UHF}(5ZaP) - E_{UHF}(4ZaP)} \right], \quad (5)$$

based on 4ZaP and 5ZaP calculations (Table III). These extrapolations are analogous to Eq.(6) and Eq.(7), respectively, in our previous paper,¹⁵ but we now employ the limit, $E_{UHF}(CBS)$, obtained from Eq.(3) above. The rms difference between these two extrapolations is less than 30 μE_h . As a further check, we can compare the CAS(10e-,8orb) energy of the $N_2 X^1\Sigma_g^+$ ground state obtained from Eq.(5), $-109.141729 E_h$, with the value obtained by application of Eq.(3) to the CAS(10e-,8orb)/5ZaP and CAS(10e-,8orb)/6ZaP energies, $-109.141713 E_h$. This suggests that the CBS limits for the CASSCF energies in Table III are accurate to about 15 μE_h .

Table III. The convergence of the CAS(10e,8orb) energies (hartree) to the CBS limit.

State	Basis Set					
	2ZaP	3ZaP	4ZaP	5ZaP	CBS[Eq.(4)]	CBS[Eq.(5)]
$X^1\Sigma_g^+$	-109.116846	-109.137445	-109.140757	-109.141570	-109.141738	-109.141729
$A^3\Sigma_u^+$	-108.886133	-108.901746	-108.903812	-108.904345	-108.904446	-108.904485
$B^3\Pi_g$	-108.829782	-108.846015	-108.848521	-108.849061	-108.849175	-108.849195
$W^3\Delta_u$	-108.827965	-108.844248	-108.846431	-108.846996	-108.847103	-108.847143
$B^3\Sigma_u^-$	-108.802217	-108.817650	-108.819676	-108.820198	-108.820300	-108.820334
$a^1\Sigma_u^-$	-108.778492	-108.794414	-108.796530	-108.797070	-108.797193	-108.797223
$a^1\Pi_g$	-108.785634	-108.802772	-108.805321	-108.805881	-108.806008	-108.806014

$w^1\Delta_u$ -108.764493 -108.781149 -108.783364 -108.783922 -108.784060 -108.784078

C. The MP2 correlation energy

The basis set convergence of the MP2 correlation energy is the best understood part of the dependence of the correlation energy on the one-electron basis set.^{42-45,11} The same spin, $\alpha\alpha$ - and $\beta\beta$ -pair energies converge²¹ with the maximum angular momentum included in the basis set, ℓ_{\max} , as ℓ_{\max}^{-5} (Fig. 2).⁴³ This behavior can be used to construct linear extrapolations of these pair correlation energies based on 3ZaP and 5ZaP MP2 calculations:

$$\sum_{i,j}^{occ} \alpha\alpha e_{ij}^{(2)}(CBS) \cong \sum_{i,j}^{occ} \alpha\alpha e_{ij}^{(2)}(5ZaP) + \frac{(5+1)^{-5}}{(3+1)^{-5} - (5+1)^{-5}} \left\{ \sum_{i,j}^{occ} \alpha\alpha e_{ij}^{(2)}(5ZaP) - \sum_{i,j}^{occ} \alpha\alpha e_{ij}^{(2)}(3ZaP) \right\}, \quad (6)$$

or based on 4ZaP and 6ZaP MP2 calculations:

$$\sum_{i,j}^{occ} \alpha\alpha e_{ij}^{(2)}(CBS) \cong \sum_{i,j}^{occ} \alpha\alpha e_{ij}^{(2)}(6ZaP) + \frac{(6+1)^{-5}}{(4+1)^{-5} - (6+1)^{-5}} \left\{ \sum_{i,j}^{occ} \alpha\alpha e_{ij}^{(2)}(6ZaP) - \sum_{i,j}^{occ} \alpha\alpha e_{ij}^{(2)}(4ZaP) \right\}. \quad (7)$$

where we have employed ℓ_0 and ℓ_0+2 to improve the stability of numerical derivatives. The rms difference between these two extrapolations is less than 50 μE_h for the eight low-lying states of N_2 (Table IV). This is clearly an overestimate of the error in Eq.(7), which is obviously the better of the two extrapolations. We would estimate our cumulative error from the UHF and the $\alpha\alpha$ -pair energies to be on the order of 20 μE_h .

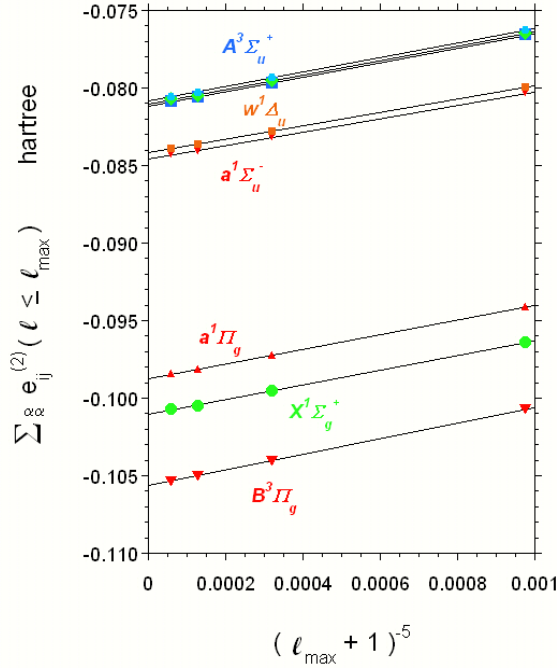


Fig. 2 The second-order $\alpha\alpha$ -pair energies converge as $(\ell_{\max}+1)^{-5}$.

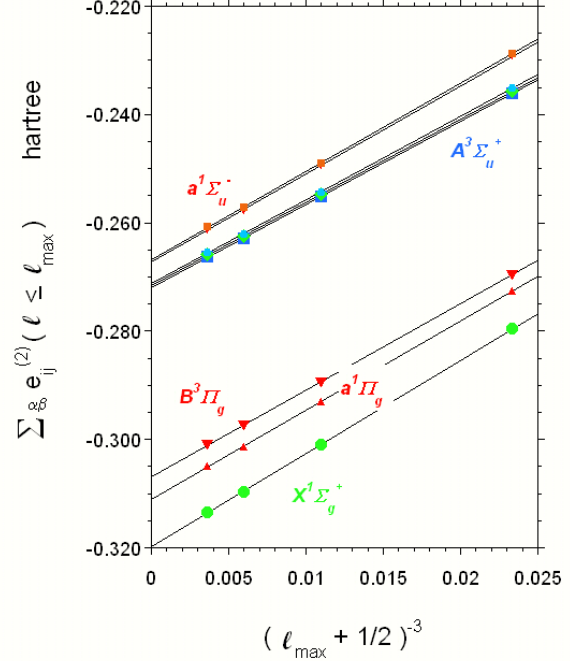


Fig. 3 The second-order $\alpha\beta$ -pair energies converge as $(\ell_{\max}+1/2)^{-3}$.

Table IV. The convergence of the sum of the second-order $\alpha\alpha$ - and $\beta\beta$ -pair energies (hartree) to the CBS limit.

State	Basis Set						CBS[Eq.(6)]	CBS[Eq.(7)]
	2ZaP	3ZaP	4ZaP	5ZaP	6ZaP			
$X^1\Sigma_g^+$	-0.083498	-0.096374	-0.099519	-0.100451	-0.100719	-0.101069	-0.100994	
$A^3\Sigma_u^+$	-0.064090	-0.076547	-0.079629	-0.080574	-0.080842	-0.081185	-0.081119	
$B^3\Pi_g$	-0.087148	-0.100655	-0.104006	-0.105020	-0.105313	-0.105682	-0.105612	
$W^3\Delta_u$	-0.063955	-0.076423	-0.079508	-0.080453	-0.080721	-0.081064	-0.080998	
$B^3\Sigma_u^-$	-0.063745	-0.076231	-0.079320	-0.080266	-0.080534	-0.080877	-0.080811	
$a^1\Sigma_u^-$	-0.069115	-0.080293	-0.083138	-0.084018	-0.084265	-0.084582	-0.084522	
$a^1\Pi_g$	-0.081801	-0.094071	-0.097211	-0.098151	-0.098423	-0.098700	-0.098700	
$w^1\Delta_u$	-0.068683	-0.079897	-0.082750	-0.083630	-0.083877	-0.084196	-0.084135	

The opposite spin, $\alpha\beta$ -pair energies, converge with the maximum angular momentum included in the basis set, ℓ_{\max} , as ℓ_{\max}^{-3} (Fig. 3).⁴² This behavior can again be used to construct linear extrapolations of these pair correlation energies based on 3ZaP and 5ZaP MP2 calculations:

$$\sum_{i,j}^{occ} \alpha\beta e_{ij}^{(2)}(CBS) \cong \sum_{i,j}^{occ} \alpha\beta e_{ij}^{(2)}(5ZaP) + \frac{(5+1/2)^{-3}}{(3+1/2)^{-3} - (5+1/2)^{-3}} \left\{ \sum_{i,j}^{occ} \alpha\beta e_{ij}^{(2)}(5ZaP) - \sum_{i,j}^{occ} \alpha\beta e_{ij}^{(2)}(3ZaP) \right\}, \quad (8)$$

or based on 4ZaP and 6ZaP MP2 calculations:

$$\sum_{i,j}^{occ} \alpha\beta e_{ij}^{(2)}(CBS) \cong \sum_{i,j}^{occ} \alpha\beta e_{ij}^{(2)}(6ZaP) + \frac{(6+1/2)^{-3}}{(4+1/2)^{-3} - (6+1/2)^{-3}} \left\{ \sum_{i,j}^{occ} \alpha\beta e_{ij}^{(2)}(6ZaP) - \sum_{i,j}^{occ} \alpha\beta e_{ij}^{(2)}(4ZaP) \right\}. \quad (9)$$

The rms difference between these two extrapolations is 447 microhartree for the eight low-lying states of N_2 (Table V). This is undoubtedly an overestimate of the error in Eq.(9), which is obviously the better of the two extrapolations. A more realistic estimate of the error comes from comparison of the total $E^{(2)}$ estimated from Eq.(7) and Eq.(9) with the value obtained from pair natural orbital (PNO) extrapolations¹¹ from the 6ZaP calculations with $N_{\min}=25$.⁴⁶ The rms deviation between the PNO extrapolations and the values for $E^{(2)}$ from Eq.(7) and Eq.(9) is 140 μE_h for the eight low-lying states of N_2 (Table V). If we adopt this figure for the error in the $\alpha\beta$ -pair extrapolation, our cumulative error is now about 150 μE_h , and comes primarily from the uncertainty in the CBS limit for the $\alpha\beta$ -pair energies.

Table V. The convergence of the sum of the second-order $\alpha\beta$ -pair energies (hartree) to the CBS limit.

State	Basis Set						CBS[Eq.(8)]	CBS[Eq.(9)]
	2ZaP	3ZaP	4ZaP	5ZaP	6ZaP			
$X^1\Sigma_g^+$	-0.228800	-0.279590	-0.300933	-0.309602	-0.313483	-0.320021	-0.319716	
$A^3\Sigma_u^+$	-0.189548	-0.235962	-0.255105	-0.262850	-0.266218	-0.272184	-0.271737	
$B^3\Pi_g$	-0.221250	-0.269528	-0.289404	-0.297457	-0.300946	-0.307153	-0.306678	
$W^3\Delta_u$	-0.189170	-0.235617	-0.254772	-0.262519	-0.265891	-0.271859	-0.271412	
$B^3\Sigma_u^-$	-0.188582	-0.235081	-0.254256	-0.262007	-0.265383	-0.271355	-0.270909	
$a^1\Sigma_u^-$	-0.179498	-0.229200	-0.249443	-0.257624	-0.261188	-0.267492	-0.267021	
$a^1\Pi_g$	-0.223270	-0.272617	-0.293068	-0.301375	-0.304964	-0.311358	-0.310871	
$w^1\Delta_u$	-0.178884	-0.228657	-0.248928	-0.257116	-0.260688	-0.266996	-0.266528	

D. The CCSD(T) energy

It is useful at this point to examine the basis set convergence of the CCSD(T) energy. The major component of the CCSD(T) correlation energy is the CCSD component. This is the part that is responsible for the proper dissociation of single bonds. However, we shall first treat the triple excitation component, since this fits the pattern of the MP2 convergence.

The increment to the correlation energy resulting from triple excitations is relatively easy to understand and extrapolate. The triple excitation energy component is dominated by the contributions from mixed spins: $\alpha\alpha\beta$, $\alpha\beta\alpha$, $\beta\alpha\alpha$, $\alpha\beta\beta$, $\beta\alpha\beta$, and $\beta\beta\alpha$. The convergence of these terms is controlled by the opposite spin interactions and thus converges as ℓ_{\max}^{-3} (Fig. 4). Once again we compare two extrapolations:

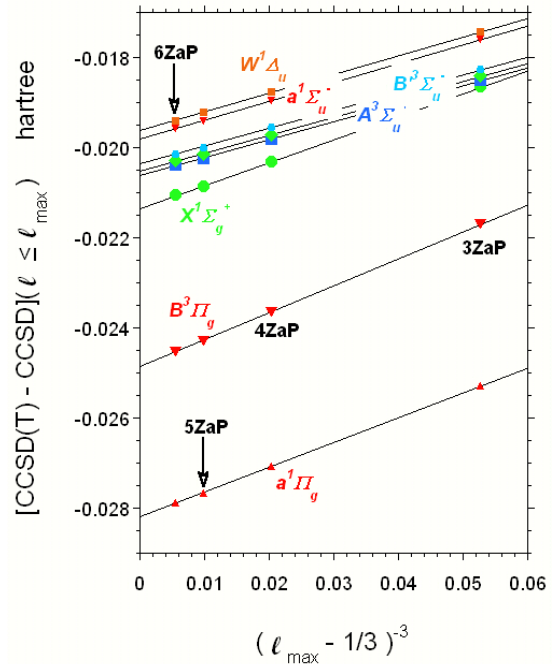


Fig. 4 The triple excitation component of the CCSD(T) energy converges as $(\ell_{\max}-1/3)^{-3}$

$$E_T(\text{CBS}) \cong E_T(5\text{ZaP}) + \frac{(5-1/3)^{-3}}{(3-1/3)^{-3} - (5-1/3)^{-3}} \{E_T(5\text{ZaP}) - E_T(3\text{ZaP})\}, \quad (10)$$

and:

$$E_T(\text{CBS}) \cong E_T(6\text{ZaP}) + \frac{(6-1/3)^{-3}}{(4-1/3)^{-3} - (6-1/3)^{-3}} \{E_T(6\text{ZaP}) - E_T(4\text{ZaP})\}. \quad (11)$$

Partly as a consequence of the modest total contribution from triple excitations, these two estimates of the CBS limit (Table VI) agree to within 30 μE_h , suggesting that any errors from Eq.(11) add something on the order of 10 μE_h to the error in our estimate of the CCSD(T) CBS limit.

The CBS limit for the CCSD component presents a greater challenge. The CCSD increment to the correlation energy (i.e. $E_{\text{CCSD}} - E_{\text{MP2}}$) becomes less negative and can even become positive as we increase the basis set (Table VII). This arises from an “*interference effect*” between the Hartree-Fock configuration and doubly excited configurations.^{11,47} We gave a detailed derivation¹¹ and quantitative tests^{47,48} of this effect a number of years ago, so we shall just give a brief description here.

Table VI. The convergence of the triple excitation component of the CCSD(T) energies (hartree) to the CBS limit.

State	Basis Set						CBS[Eq.(10)]	CBS[Eq.(11)]
	2ZaP	3ZaP	4ZaP	5ZaP	6ZaP			
X $^1\Sigma_g^+$	-0.012542	-0.018646	-0.020311	-0.020858	-0.021044	-0.021366	-0.021317	
A $^3\Sigma_u^+$	-0.014222	-0.018509	-0.019806	-0.020239	-0.020391	-0.020635	-0.020608	
B $^3\Pi_g$	-0.015248	-0.021700	-0.023652	-0.024282	-0.024516	-0.024875	-0.024836	
W $^3\Delta_u$	-0.014135	-0.018413	-0.019708	-0.020140	-0.020292	-0.020536	-0.020509	
B $^3\Sigma_u^-$	-0.014000	-0.018264	-0.019556	-0.019987	-0.020138	-0.020382	-0.020355	
a $^1\Sigma_u^-$	-0.013383	-0.017601	-0.018952	-0.019413	-0.019581	-0.019829	-0.019816	
a $^1\Pi_g$	-0.019411	-0.025275	-0.027079	-0.027663	-0.027882	-0.028211	-0.028181	
w $^1\Delta_u$	-0.013219	-0.017419	-0.018764	-0.019224	-0.019391	-0.019638	-0.019625	

The wave function including double excitations within a particular basis set (e.g. 5ZaP):

$$\psi = \phi_{\text{HF}} + \sum_{i,j \text{ occ}}^{a,b \text{ virt}} C_{ij}^{ab} (5\text{ZaP}) \phi_{ij}^{ab} (5\text{ZaP}), \quad (12)$$

has coefficients, C , that are all negative. If we now expand the basis set (e.g. to 6ZaP), the increment to the second-order correlation energy is:

Table VII. The convergence of the CCSD – MP2 component of the correlation energies (hartree) to the CBS limit.

State	Basis Set						CBS[Eq.(17)]	CBS[Eq.(18)]
	2ZaP	3ZaP	4ZaP	5ZaP	6ZaP			
$X^1\Sigma_g^+$	-0.002121	0.002177	0.006062	0.008805	0.010302	0.013044	0.013069	
$A^3\Sigma_u^+$	-0.028402	-0.023780	-0.019883	-0.017276	-0.015881	-0.013588	-0.013475	
$B^3\Pi_g$	-0.004908	-0.000398	0.003463	0.006095	0.007492	0.010230	0.010211	
$W^3\Delta_u$	-0.028451	-0.023847	-0.019958	-0.017353	-0.015960	-0.013669	-0.013555	
$B^3\Sigma_u^-$	-0.028525	-0.023948	-0.020072	-0.017472	-0.016079	-0.013792	-0.013677	
$a^1\Sigma_u^-$	-0.029860	-0.026127	-0.022501	-0.019901	-0.018492	-0.016242	-0.016100	
$a^1\Pi_g$	-0.013336	-0.008720	-0.004712	-0.001975	-0.000527	0.001939	0.002054	
$w^1\Delta_u$	-0.029965	-0.026256	-0.022642	-0.020046	-0.018637	-0.016390	-0.016247	

$$\Delta E^{(2)} = \sum_{i,j occ}^{\mu,\nu virt} \frac{\left| \langle \phi_{HF} | r_{12}^{-1} | \phi_{ij}^{\mu\nu}(\mu,\nu \text{ in } 6ZaP) \rangle \right|^2}{\epsilon_i + \epsilon_j - \epsilon_\mu - \epsilon_\nu}. \quad (13)$$

However, to second-order the increment in the CCSD correlation energy is:

$$\Delta E_{CCSD} = \sum_{i,j occ}^{\mu,\nu virt} \frac{\left| \langle \phi_{HF} + \sum C_{ij}^{ab} (5ZaP) \phi_{ij}^{ab} (5ZaP) | r_{12}^{-1} | \phi_{ij}^{\mu\nu}(\mu,\nu \text{ in } 6ZaP) \rangle \right|^2}{\epsilon_i + \epsilon_j - \epsilon_\mu - \epsilon_\nu}, \quad (14)$$

Where we have included all configurations in Eq.(12). We have shown^{11,47} that in the limit as μ and ν approach ∞ , all matrix elements in Eq.(14) approach the same value:

$$\Delta E_{CCSD} \cong \left[1 + \sum_{i,j occ}^{a,b virt} C_{ij}^{ab} (a,b \text{ in } 5ZaP) \right]^2 \times \sum_{i,j occ}^{\mu,\nu virt} \frac{\left| \langle \phi_{HF} | r_{12}^{-1} | \phi_{ij}^{\mu\nu}(\mu,\nu \text{ in } 6ZaP) \rangle \right|^2}{\epsilon_i + \epsilon_j - \epsilon_\mu - \epsilon_\nu}, \quad (15)$$

so the basis set change to the CCSD increment to the correlation energy is:⁴⁹

$$\Delta E_{CCSD} - \Delta E^{(2)} \cong \left\{ \left[1 + \sum_{i,j occ}^{a,b virt} C_{ij}^{ab} (a,b \text{ in } 5ZaP) \right]^2 - 1 \right\} \times \Delta E^{(2)}, \quad (16)$$

which will always be positive (Table VII). The CCSD increment given by Eq.(16) is available (as: ‘‘CBS-int’’) from the CBS PNO extrapolation code that we have implemented in the Gaussian suite of programs.³³

We shall again compare two levels of extrapolation to provide a measure of the accuracy of the CCSD/CBS correlation energy:

$$E_{CCSD}(CBS) \cong E_{CCSD}(5ZaP) + \Delta E_{CBS-int}(5ZaP, N \text{ min} = 20), \quad (17)$$

and:

$$E_{CCSD}(CBS) \cong E_{CCSD}(6ZaP) + \Delta E_{CBS-int}(6ZaP, N \text{ min} = 25). \quad (18)$$

The correction to the CCSD/6ZaP energy is about 2.5 mE_h, but the rms deviation between these two estimates is only 109 μE_h. We again note that the error from the better estimate is certainly considerably smaller than this, perhaps about 30 μE_h.

If we now consider the cumulative effects from errors in our estimates of the CBS limits for the UHF (10 μE_h), MP2(αα) (20 μE_h), MP2(αβ) (140 μE_h), CCSD (30 μE_h), and CCSD(T) (10 μE_h) energies, we estimate the accuracy of our extrapolated CCSD(T)/CBS limit to be about 200 μE_h. This is consistent with the rms difference between the sum of our 5ZaP extrapolations (Tables II, IV, V, VI, and VII) and the sum of our 6ZaP extrapolations (638 μE_h).

E. The CAS-CISD energy

We are finally ready to consider the basis set convergence of the CISD correction to the CAS(10e,8orb) energy (Table VIII). Just as the basis set convergence of the UHF energy provided a model for the basis set convergence of the CAS energy, the UCCSD dynamic correlation energy provides a model for the basis set convergence of the CAS-CISD dynamic correlation energy (Fig. 5). Several plausible candidates for modeling the

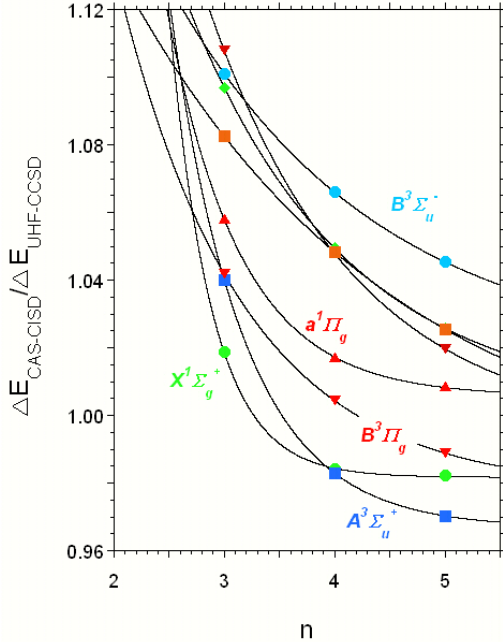
Table VIII. The convergence of the CAS(10e,8orb)-CISD dynamic correlation energies (hartree) to the CBS limit.

State	Basis Set					
	2ZaP	3ZaP	4ZaP	5ZaP	CBS[4ZaP]	CBS[5ZaP]
X ¹ Σ _g ⁺	-0.173425	-0.233904	-0.254180	-0.260915	-0.267218	-0.267194
A ³ Σ _u ⁺	-0.189401	-0.245821	-0.263836	-0.269738	-0.275349	-0.275090
B ³ Π _g	-0.194374	-0.254043	-0.273493	-0.279857	-0.285677	-0.285353
W ³ Δ _u	-0.196363	-0.255934	-0.275193	-0.281438	-0.287500	-0.287015
B' ³ Σ _u ⁻	-0.192829	-0.252737	-0.272337	-0.278710	-0.284861	-0.284438
a' ¹ Σ _u ⁻	-0.201940	-0.265248	-0.285640	-0.292229	-0.298803	-0.298184
a ¹ Π _g	-0.192215	-0.252535	-0.272454	-0.279017	-0.285193	-0.285003
w ¹ Δ _u	-0.198701	-0.260704	-0.281157	-0.287794	-0.294356	-0.293851

CAS-CISD convergence have been considered. The UHF-CISD, CAS-CISD, CCSD, and CCSD(T) methods are all equivalent to a full CI for two electrons. The full valence CAS we have employed in this paper reduces to a single configuration Hartree-Fock for a species such as Neon with all valence orbitals fully occupied. Thus, UHF-CISD would be the correct model in the two limiting cases of Li_2 and Ne_2 . However, the lack of disconnected quadruple and higher excitations (i.e. linked diagrams) makes UHF-CISD an inappropriate model for a CAS-CISD calculation of N_2 , which includes the most important quadruple excitations.

Thus, it is not surprising that CCSD closely mimics the basis set convergence of CAS-CISD. The ratio of $\Delta E_{\text{CAS-CISD}}$ to ΔE_{CCSD} :

$$\rho_n \equiv \frac{\{E_{\text{CAS-CISD}}(n\text{ZaP}) - E_{\text{CAS}}(n\text{ZaP})\} - \{E_{\text{CAS-CISD}}(\{n-1\}\text{ZaP}) - E_{\text{CAS}}(\{n-1\}\text{ZaP})\}}{\{E_{\text{CCSD}}(n\text{ZaP}) - E_{\text{UHF}}(n\text{ZaP})\} - \{E_{\text{CCSD}}(\{n-1\}\text{ZaP}) - E_{\text{UHF}}(\{n-1\}\text{ZaP})\}}, \quad (19)$$



is very close to unity, but shows a small systematic decrease with increasing n (Fig. 6), approaching limiting values between 0.96 and 1.02 for the various states. We can use this pattern to estimate the ratio for larger basis sets:

$$\rho_{n+1} \cong \rho_n \left(\frac{\rho_n}{\rho_{n-1}} \right). \quad (20)$$

Fig. 6 The ratio of the basis set increments of the CAS-CISD dynamic correlation energy to the CCSD dynamic correlation energy [Eq.(19)] decreases monotonically as the basis set increases. The exponential curves satisfy Eq.(20).

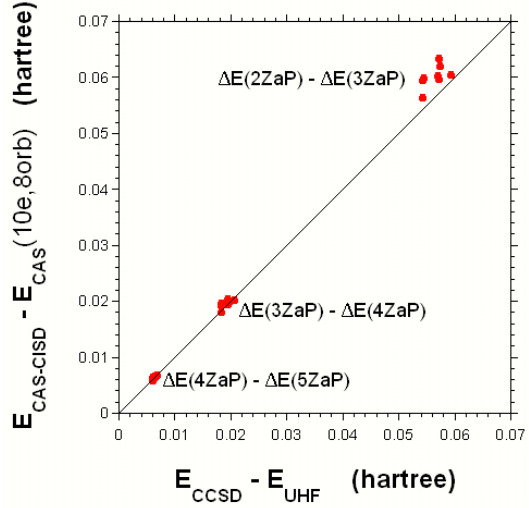


Fig. 5 The basis set increments in the CCSD dynamic correlation energy very nearly equal the basis set increments in the CAS-CISD dynamic correlation energy.

The combination of Eq.(20) with Eq.(19) gives the extrapolation formula for $E_{\text{CAS-CISD}}$ that was used in Table VIII:

$$\begin{aligned} \Delta E_{\text{CAS-CISD}}(n+1) &\cong \rho_n \left(\frac{\rho_n}{\rho_{n-1}} \right) \Delta E_{\text{CCSD}}(n+1) , \\ \Delta E_{\text{CAS-CISD}}(n+2) &\cong \rho_n \left(\frac{\rho_n}{\rho_{n-1}} \right)^2 \Delta E_{\text{CCSD}}(n+2) , \text{ etc.} \end{aligned} \tag{21}$$

The rms difference between the extrapolations based on 4ZaP and 5ZaP calculations is less than 400 μE_h (Table VIII). We estimate the accuracy of our extrapolated CAS-CISD(5ZaP)/CBS limit to be about 200 μE_h . The only way to test this estimate is to calculate the core and core-valence contributions to the correlation energy and estimate the full CI correction to the CAS-CISD energy so we can compare our calculations to experiment.

F. Full configuration interaction

Bytautas and Ruedenberg have recently examined the convergence of full CI energies with the cc-pVnZ basis sets.⁵⁰ Their results for the $X^1\Sigma_g^+$ ground state of N_2 at 1.0977 Å are included in Table IX. We observe that in this particular example the CCSD(T) energy differs from the FCI energy by less than 2 mE_h for all three basis sets for which results are available and that this small difference slowly decreases with increasing basis set. In fact, the basis set increment to this difference, $\Delta[\text{FCI-CCSD(T)}]$, follows the basis set increment to the CCSD(T) correlation energy, $\Delta[\text{CCSD(T)-SCF}]$, the ratio being -0.004. If we assume that this ratio persists, we can estimate the changes to $\Delta[\text{FCI-CCSD(T)}]$, and thus the FCI energy with the larger basis sets and the FCI/CBS limit (the CCSD(T)/CBS limit was extrapolated as described above). Our extrapolated FCI/CBS limit (-109.42363) is in excellent agreement with the “experimental” valence FCI energy given by Bytautas and Ruedenberg (-109.4237 E_h).⁵⁰

The FCI energies in the last row of Table IX were used to obtain the FCI corrections to the CAS(10,8)-CISD energies of the $X^1\Sigma_g^+$ N_2 ground state as given in Table X. We have also included FCI/cc-pVDZ corrections for the $a^1\Sigma_u^-$, $a^1\Pi_g$, and $w^1\Delta_u$ excited states obtained from the FCI calculations of Larsen, Olsen, and Jørgensen.⁵¹ We employed a linear interpolation of $\Delta E(\text{R}_{\text{NN}})$ to obtain ΔE at the geometries in Table I. The remaining values in Table X are based on two reasonable approximations that are best justified by the ultimate agreement with experiment (*vide infra*). Since we did not have FCI energies for the triplet states, we assumed that the FCI correction for the triplet states

Table IX. The basis set convergence of the FCI energy for the $X^1\Sigma_g^+$ ground state of N_2 .

Energy Component	cc-pVDZ	cc-pVTZ	cc-pVQZ	cc-pV5Z	cc-pV6Z	CBS limit
SCF	-108.954128	-108.983470	-108.991084	-108.992765	-108.993086	-108.993185
CCSD(T)	-109.275253	-109.373840	-109.404373	-109.414187	-109.417772	-109.422333
CCSD(T)-SCF	-0.321125	-0.390370	-0.413289	-0.421422	-0.424686	-0.429148
$\Delta[CCSD(T)-SCF]$		-0.062624	-0.021236	-0.007498	-0.003032	-0.004097
FCI ^a	-109.27698	-109.37530	-109.40573			
FCI-CCSD(T)	-0.00173	-0.00146	-0.00136			
$\Delta[FCI-CCSD(T)]$		0.00027	0.00010			
$\Delta[FCI-CCSD(T)]$ $\Delta[CCSD(T)-SCF]$		-0.0039	-0.004			
-0.004 x $\Delta[CCSD(T)-SCF]$		0.00028	0.00009	0.00003	0.00001	0.00002
{FCI-CCSD(T)}(cc-pVDZ) -0.004 x $\Delta[CCSD(T)-SCF]$		-0.00145	-0.00136	-0.00133	-0.00131	-0.00130
CCSD(T)+{FCI-CCSD(T)}(cc-pVDZ) -0.004 x $\Delta[CCSD(T)-SCF]$ ^b		-109.375290	-109.405732	-109.415513	-109.419085	-109.423628

a. Reference 50.

b. Our extrapolation of the FCI energies.

Table X. The basis set convergence of the FCI correction to the CAS(10e,8orb)-CISD energies (hartree).

State	Basis Set				CBS
	cc-pVDZ	cc-pVTZ	cc-pVQZ	cc-pV5Z	
$X^1\Sigma_g^+$	-0.005780 ^a	-0.01128 ^a	-0.01314 ^a	-0.01393	-0.014710 ^d
$A^3\Sigma_u^+$	-0.006908 ^c				-0.016983 ^d
$B^3\Pi_g$	-0.007191 ^c				-0.018082 ^d
$W^3\Delta_u$	-0.007221 ^c				-0.018078 ^d
$B'^3\Sigma_u^-$	-0.007145 ^c				-0.018040 ^d
$a^1\Sigma_u^-$	-0.007492 ^b				-0.019066 ^d
$a^1\Pi_g$	-0.007183 ^b				-0.018281 ^d
$w^1\Delta_u$	-0.007394 ^b				-0.018818 ^d

a. Ref. 50. b. Ref. 51 c. Estimated from b. d. 2.545 x cc-pVDZ

was the same fraction of the CAS-CISD dynamic correlation energy as was found for the corresponding singlet states (e.g. $B^3\Pi_g$ vs $a^1\Pi_g$). We then made the further assumption that the ratio of the complete basis set correction to the cc-pVDZ correction was the same for the excited states as for the ground state (i.e. 2.545). The differences in these FCI corrections for the different states are modest, but our justification for this assumption lies primarily in the accuracy of the excitation energies that result (*vide infra*). We shall apply the cc-pVnZ corrections from Table X to our nZaP CAS-CISD calculations.

G. Core electrons

We have calculated the core-core and core-valence effects on the correlation energy using several basis sets (Table XI). The first is the standard APNO kk, kl, ll basis set⁵² included in Gaussian.TM The 3ZaPcore and 4ZaPcore basis sets include additional basis functions that were optimized for the MP2 energy of the 1s electrons plus functions with intermediate exponents. The core correlation energies in Table XI were obtained from pair natural orbital extrapolations^{11,52} using a minimum of 5, 10, and 15 PNOs for the APNO, 3ZaPcore, and 4ZaPcore basis sets respectively. The variations in the core effects for the various states are modest. The rms change in the core contribution to the excitation energies is 118 μE_h between the APNO and 3ZaPcore basis sets and 27 μE_h between the 3ZaPcore and 4ZaPcore basis sets. These small changes and the agreement of our ground state results with the CCSD(T)-R12 results of Noga, Valiron, and Klopper⁵³ indicate that the accuracy of the 4ZaPcore calculations is sufficient for our purposes.

Table XI. The CBS extrapolated core-core, core-valence correlation energies (hartree).

State	APNO/CBS	3ZaPcore	4ZaPcore	CCSD(T)-R12 ^a
N $^4S_{3/2}$	-0.057073	-0.058140	-0.058474	-0.058779
X $^1\Sigma_g^+$	-0.116085	-0.117978	-0.118618	-0.118983
A $^3\Sigma_u^+$	-0.114834	-0.116682	-0.117350	
B $^3\Pi_g$	-0.115596	-0.117294	-0.117954	
W $^3\Delta_u$	-0.114854	-0.116703	-0.117371	
B ³ $^3\Sigma_u^-$	-0.115073	-0.116733	-0.117402	
a ¹ $^1\Sigma_u^-$	-0.114665	-0.116548	-0.117217	
a $^1\Pi_g$	-0.115109	-0.117045	-0.117710	
w $^1\Delta_u$	-0.114714	-0.116597	-0.117266	

a. Reference 53.

H. Total energies

We can now assemble all the components necessary for comparison with experiment. We combine the CAS(10e⁻,8orb) energies from Table III with the CISD corrections from Table VIII, the full CI corrections from Table X, and the core contributions from Table XI to obtain the total energies at the geometries, R_e, from Table I. These total energies yield the equilibrium geometry excitation energies, T_e, given in Table XII. The excellent agreement of these excitation energies with experiment provides justification for the assumptions made in Section III. F. about the convergence of the full CI corrections, but the real significance lies in the validation of the accuracy of the extrapolated CAS-CISD/CBS limits, which are the focus of this study.

Table XII. Calculated and experimental excitation energies, T_e (eV), at experimental R_e.^a

State	CAS(10,8)-CISD				CBS ^b	+ FCI ^c	+ core ^d	Exp. ^a
	2ZaP	3ZaP	4ZaP	5ZaP				
X ¹ Σ _g ⁺ → A ³ Σ _u ⁺	5.843	6.089	6.185	6.215	6.240	6.179	6.213	6.224
→ B ³ Π _g	7.241	7.382	7.427	7.444	7.466	7.374	7.392	7.392
→ W ³ Δ _u	7.237	7.379	7.437	7.457	7.476	7.376	7.410	7.415
→ B ³ Σ _u ⁻	8.034	8.190	8.243	8.261	8.276	8.182	8.215	8.217
→ a ¹ Σ _u ⁻	8.431	8.482	8.511	8.522	8.531	8.412	8.450	8.450
→ a ¹ Π _g	8.501	8.600	8.630	8.642	8.650	8.553	8.578	8.590
→ w ¹ Δ _u	8.900	8.966	8.991	9.001	9.006	8.895	8.931	8.939
Rms error	0.186	0.056	0.041	0.051	0.063	0.038	0.007	

a. Reference 32. b. Sum of the last column of Table III plus the last column of Table VIII.

c. Sum of the previous column plus the last column of Table X.

d. Sum of the previous column plus the 4ZaPcore column of Table XI.

IV. RESULTS

Excitation energies measure the relationship between the potential energy surfaces of different states. We must also consider predicted equilibrium geometries and harmonic and anharmonic vibrational constants as measures of the short-range accuracy of the individual potential energy surfaces, along with dissociation energies as measures of the long-range accuracy of these surfaces. We have therefore repeated the above calculations at 7 points on a 0.01Å grid for each of the 8 states of N₂ under study. A polynomial of degree 5 was least-squares fit to the 7 grid points to determine R_e, ω_e, and ω_eX_e for each of the 8 states of N₂. The values of R_e and ω_e were consistently well-defined, but the third- and especially the fourth- derivatives were problematic for the

most elaborate calculations (*vide infra*). The dissociation energies were determined both from calculations at 20 Å and also from calculations on the atomic $^4S_{3/2}$, $^2D_{3/2}$ and $^2P_{1/2}$ states.

A. Equilibrium geometries

The CAS(10e-,8orb), CAS(10e-,8orb)-CISD, CAS(10e-,8orb)-CISD + FCI correction, and CAS(10e-,8orb)-CISD + FCI correction + core-core & core valence optimized geometries are compared to the experimental geometries in Table XIII. The CAS/2ZaP geometries are comparable to the CAS-CISD/2ZaP geometries, but the CAS geometries do not improve significantly beyond the 3ZaP basis set and are consistently about 0.012 Å too long, whereas the CAS-CISD/CBS geometries are within 0.0016 Å of the experimental values. FCI corrections to the CAS-CISD energies lengthen the bonds by about 0.0008 Å and core effects then reduce the bond lengths to within 0.0005 Å of the experimental values

Table XIII. Calculated and experimental equilibrium geometries, R_e (Å).

State	CAS(10,8)			CAS(10,8)-CISD					+ FCI	+ core	Exp. ^a
	2ZaP	3ZaP	CBS	2ZaP	3ZaP	4ZaP	5ZaP	CBS			
X $^1\Sigma_g^+$	1.1148	1.1060	1.1036	1.1181	1.1054	1.1019	1.1008	1.0998	1.1000	1.0977	1.0977
A $^3\Sigma_u^+$	1.3069	1.3023	1.3006	1.3067	1.2962	1.2920	1.2907	1.2884	1.2893	1.2863	1.2866
B $^3\Pi_g$	1.2320	1.2268	1.2246	1.2314	1.2209	1.2169	1.2156	1.2138	1.2145	1.2119	1.2126
W $^3\Delta_u$	1.2980	1.2936	1.2920	1.2973	1.2879	1.2844	1.2833	1.2812	1.2824	1.2795	
B' $^3\Sigma_u^-$	1.2984	1.2939	1.2922	1.2962	1.2863	1.2827	1.2816	1.2795	1.2804	1.2775	1.278 ₄
a' $^1\Sigma_u^-$	1.2927	1.2882	1.2866	1.2917	1.2826	1.2796	1.2786	1.2768	1.2779	1.2750	1.2755
a $^1\Pi_g$	1.2395	1.2343	1.2321	1.2392	1.2292	1.2252	1.2240	1.2221	1.2227	1.2202	1.2203
w $^1\Delta_u$	1.2865	1.2821	1.2805	1.2845	1.2755	1.2724	1.2714	1.2696	1.2708	1.2679	1.268
Rms error	0.0189	0.0137	0.0119	0.0185	0.0082	0.0046	0.0034	0.0016	0.0024	0.0005	

a. Reference 32.

B. Harmonic vibrational frequencies

The calculated harmonic vibrational frequencies are given in Table XIV. Once again, the CAS/2ZaP results are comparable to the CAS-CISD/2ZaP results, but the CAS frequencies do not improve with larger basis sets. If we scale the CAS/2ZaP and CAS-CISD/2ZaP frequencies by 1.015, the rms errors are reduced to 14.1 cm^{-1} and 7.9 cm^{-1} respectively. When full CI and core corrections are added to the CAS-CISD/CBS

energies, the harmonic vibrational frequencies increase to within 2.3 cm^{-1} of the experimental values.

Table XIV. Calculated and experimental harmonic vibrational frequencies, ω_e (cm^{-1}).

State	CAS(10,8)			CAS(10,8)-CISD					+ FCI	+ core	Exp. ^a
	2ZaP	3ZaP	CBS	2ZaP	3ZaP	4ZaP	5ZaP	CBS			
$X^1\Sigma_g^+$	2344.6	2337.1	2340.6	2320.6	2332.1	2342.6	2346.0	2349.1	2346.3	2356.3	2358.57
$A^3\Sigma_u^+$	1421.6	1420.4	1420.0	1419.3	1435.9	1446.6	1450.0	1458.5	1452.3	1464.3	1460.64
$B^3\Pi_g$	1706.5	1694.7	1696.1	1707.6	1712.4	1723.0	1726.2	1732.4	1725.7	1735.6	1733.39
$W^3\Delta_u$	1476.9	1472.5	1471.0	1481.8	1489.2	1495.9	1498.1	1505.1	1497.7	1503.6	1501.4
$B^3\Sigma_u^-$	1476.8	1472.4	1470.8	1491.8	1501.2	1508.0	1510.2	1517.3	1511.2	1516.2	1516.88
$a^1\Sigma_u^-$	1501.8	1496.6	1494.8	1512.3	1517.6	1522.2	1523.7	1531.6	1526.4	1533.4	1530.25
$a^1\Pi_g$	1687.2	1675.8	1676.8	1674.2	1675.2	1684.4	1687.3	1694.2	1682.9	1693.4	1694.21
$w^1\Delta_u$	1524.7	1518.6	1516.3	1541.9	1547.7	1552.0	1553.4	1558.0	1551.7	1560.7	1559.26
Rms error	28.9	34.5	35.1	27.1	18.7	10.5	7.9	3.7	8.1	2.3	

a. Reference 32.

C. Anharmonic constants

The CAS results (Table XV) show the familiar pattern of no improvement beyond the 2ZaP basis set. However, the CAS-CISD anharmonic constants also show no improvement beyond the 3ZaP basis set. The erratic pattern with larger basis sets suggests that the CAS-CISD calculations with basis sets beyond 3ZaP are not sufficiently

Table XV. Calculated and experimental anharmonic constants, $\omega_e X_e$ (cm^{-1}).

State	CAS(10,8)			CAS(10,8)-CISD					+ FCI	+ core	Exp. ^a
	2ZaP	3ZaP	CBS	2ZaP	3ZaP	4ZaP	5ZaP	CBS			
$X^1\Sigma_g^+$	13.0	13.5	13.6	13.3	14.0	13.3	13.2	13.0	12.0	11.5	14.324
$A^3\Sigma_u^+$	14.0	13.3	13.3	14.1	13.6	13.6	13.6	13.4	13.1	10.1	13.872
$B^3\Pi_g$	13.0	12.8	13.0	13.4	13.6	13.9	14.0	14.1	15.7	14.8	14.122
$W^3\Delta_u$	12.2	11.6	11.6	10.9	12.0	12.6	12.7	12.9	14.7	11.6	11.6
$B^3\Sigma_u^-$	11.7	11.2	11.2	11.9	11.6	11.3	11.5	11.2	11.7	8.9	12.181
$a^1\Sigma_u^-$	12.2	11.5	11.5	12.2	12.1	12.0	12.0	11.8	10.0	13.1	12.075
$a^1\Pi_g$	12.2	11.9	12.1	13.0	13.7	13.5	13.4	13.2	14.4	13.8	13.949
$w^1\Delta_u$	11.8	11.1	11.1	11.9	11.6	11.0	10.9	10.5	11.2	11.0	11.63
Rms error	0.9	1.0	0.9	0.6	0.3	0.6	0.7	0.9	1.7	2.1	

a. Reference 32.

converged to obtain meaningful fourth derivatives. Nevertheless, the rms error for the CAS-CISD/3ZaP anharmonic constants (0.3 cm^{-1}) is small compared to the range of $\omega_e X_e$ (11.6 to 14.3 cm^{-1}), indicating that our results for small basis sets are meaningful.

D. Excitation energies

We have noted that the CAS-CISD/2ZaP geometries and frequencies show little improvement over the CAS/2ZaP values (Table XIII and Table XIV). One might infer that the CAS(10e,8orb) calculation has exhausted the small 2ZaP basis set. However, the CAS-CISD/2ZaP excitation energies do show substantial improvement over the CAS/2ZaP values (Table XVI). In contrast to the geometry and frequency calculations, the CAS excitation energies are only useful for qualitative purposes. For example, the order of the $a^1\Sigma_u^-$ and $a^1\Pi_g$ states is reversed. The CAS-CISD/2ZaP excitation energies are generally too small, but the CAS-CISD values increase beyond the experimental values in the CBS limit. The full CI and core correlation corrections then bring the calculated values to within 0.007 eV of the experimental values. This close agreement with experiment verifies the accuracy of the CAS-CISD/CBS limits.

Table XVI. Calculated and experimental excitation energies, T_e (eV).

State	CAS(10,8)			CAS(10,8)-CISD					+ FCI	+ core	Exp. ^a
	2ZaP	3ZaP	CBS	2ZaP	3ZaP	4ZaP	5ZaP	CBS			
$X^1\Sigma_g^+ \rightarrow$											
A $^3\Sigma_u^+$	6.288	6.412	6.453	5.863	6.091	6.185	6.215	6.242	6.179	6.213	6.224
B $^3\Pi_g$	7.818	7.927	7.957	7.258	7.384	7.427	7.445	7.466	7.374	7.392	7.392
W $^3\Delta_u$	7.876	7.980	8.017	7.262	7.383	7.439	7.458	7.478	7.385	7.418	7.415
B $^3\Sigma_u^-$	8.571	8.700	8.743	8.055	8.192	8.244	8.261	8.277	8.186	8.218	8.217
a $^1\Sigma_u^-$	9.220	9.334	9.373	8.454	8.484	8.512	8.523	8.532	8.413	8.451	8.450
a $^1\Pi_g$	9.020	9.105	9.133	8.518	8.601	8.631	8.642	8.651	8.539	8.578	8.590
w $^1\Delta_u$	9.599	9.694	9.730	8.922	8.969	8.992	9.001	9.007	8.895	8.931	8.939
Rms error	0.498	0.597	0.631	0.171	0.055	0.042	0.051	0.064	0.036	0.007	

a. Reference 32.

E. Dissociation energies

The recent determination of the dissociation energy of the $X^1\Sigma_g^+$ ground state of N_2 to within ± 0.001 eV by Tang, Hou, Ng, and Ruscic⁵⁴ can be combined with the tabulated N_2 excitation energies³² and atomic energy levels of nitrogen⁵⁵ to give experimental dissociation energies for all eight states of N_2 with an uncertainty of ± 0.001

eV (Table XVII). Since the molecular correlation energies are larger than the sum of the atomic correlation energies, the incomplete treatment of electron correlation in CAS and CAS-CISD calculations gives dissociation energies that are consistently too small. Full CI and core corrections bring the CAS-CISD dissociation energies into close agreement with experiment (Table XVII).

Table XVII. Calculated and experimental dissociation energies, D_e (eV), using atomic calculations.

State	CAS(10,8)			CAS(10,8)-CISD					+ FCI	+ core	Exp. ^a
	2ZaP	3ZaP	CBS	2ZaP	3ZaP	4ZaP	5ZaP	CBS			
$X^1\Sigma_g^+ \rightarrow 2^4S_{3/2}$	8.874	9.171	9.249	8.689	9.277	9.515	9.593	9.673	9.867	9.905	9.900
$A^3\Sigma_u^+ \rightarrow 2^4S_{3/2}$	2.596	2.757	2.793	2.845	3.187	3.330	3.378	3.433	3.688	3.692	3.676
$B^3\Pi_g \rightarrow ^4S_{3/2} + ^2D_{3/2}$	3.911	4.090	4.132	4.120	4.404	4.529	4.566	4.592	4.851	4.899	4.892
$W^3\Delta_u \rightarrow ^4S_{3/2} + ^2D_{3/2}$	3.862	4.042	4.077	4.125	4.407	4.518	4.553	4.581	4.841	4.872	4.869
$B'^3\Sigma_u^- \rightarrow ^4S_{3/2} + ^2P_{1/2}$	4.067	4.233	4.263	4.458	4.785	4.904	4.943	4.966	5.225	5.257	5.259
$a'^1\Sigma_u^- \rightarrow 2^2D_{3/2}$	5.364	5.536	5.562	5.604	5.814	5.884	5.906	5.911	6.172	6.226	6.218
$a^1\Pi_g \rightarrow 2^2D_{3/2}$	5.559	5.763	5.801	5.534	5.695	5.765	5.786	5.792	6.031	6.098	6.078
$w^1\Delta_u \rightarrow 2^2D_{3/2}$	4.984	5.175	5.204	5.135	5.329	5.404	5.428	5.436	5.690	5.745	5.729
Rms error	0.947	0.761	0.723	0.789	0.471	0.347	0.309	0.281	0.037	0.012	

a. Reference 32, 54, and 55.

If we employ molecular calculations at 20 Å rather than atomic calculations to determine the dissociation limits, the CAS dissociation energies are unaffected, but the CAS-CISD dissociation energies are now in much better agreement with experiment (Table XVIII). The CAS-CISD/CBS limit for the dissociation energies determined this way is of comparable accuracy to the CAS-CISD/CBS limit for the excitation energies (Table XVI). This demonstrates the importance of size-consistency. The calculations in Table XVIII maintain the same number of electrons in all calculations so that size-consistency errors cancel. The residual errors of ~0.04 eV represent effects beyond simultaneous single and double excitations.

V. DISCUSSION

Having established the CAS-CISD/CBS limits, we can now use them as a guide to evaluate extrapolations based on more modest calculations. A CAS/2ZaP geometry optimization and zero-point energy calculation followed by a CAS-CISD/3ZaP single point energy calculation would give excitation energies accurate to ~0.05 eV (Table XVI). Unfortunately, this CAS-CISD/3ZaP//CAS/2ZaP model chemistry gives poor

Table XVIII. Calculated and experimental dissociation energies, D_e (eV), using molecular calculations at 20 Å.

State	CAS(10,8)-CISD					+ core	Exp. ^a
	2ZaP	3ZaP	4ZaP	5ZaP	CBS		
$X^1\Sigma_g^+ \rightarrow 2^4S_{3/2}$	8.783	9.431	9.687	9.769	9.834	9.873	9.900
$A^3\Sigma_u^+ \rightarrow 2^4S_{3/2}$	2.942	3.346	3.508	3.559	3.600	3.604	3.676
$B^3\Pi_g \rightarrow ^4S_{3/2} + ^2D_{3/2}$	4.230	4.587	4.735	4.781	4.799	4.847	4.892
$W^3\Delta_u \rightarrow ^4S_{3/2} + ^2D_{3/2}$	4.238	4.593	4.727	4.769	4.789	4.821	4.869
$B^3\Sigma_u^- \rightarrow ^4S_{3/2} + ^2P_{1/2}$	4.572	4.972	5.113	5.158	5.181	5.213	5.259
$a'^1\Sigma_u^- \rightarrow 2^2D_{3/2}$	5.727	6.016	6.113	6.144	6.148	6.202	6.218
$a^1\Pi_g \rightarrow 2^2D_{3/2}$	5.656	5.899	5.995	6.025	6.025	6.092	6.078
$w^1\Delta_u^- \rightarrow 2^2D_{3/2}$	5.269	5.534	5.633	5.664	5.669	5.724	5.729
Rms error	0.682	0.294	0.144	0.097	0.073	0.040	

a. Reference 32, 54, and 55.

accuracy (~ 0.3 eV) for dissociation energies (Table XVIII), and thus would not be a good choice for studies of reactive surfaces. The corrections to the CAS-CISD/3ZaP energy are relatively independent of the electronic state, but show a strong dependence on geometry.

The CAS-CISD/3ZaP calculations describe the local behavior of a potential energy surface (i.e. R_e , ω_e , $\omega_e X_e$, and T_e) with sufficient accuracy for most purposes (Tables XIII – XVI), and thus provide an appropriate starting point for a model chemistry. However, the long range behavior (i.e. D_e) requires large basis sets or extrapolations to the CBS limit (Table XVIII). The development of a reliable extrapolation scheme will require careful testing on a variety of examples. Nevertheless, the results we have are sufficient to suggest a preliminary model for reactive surfaces. We shall employ the same mathematical models described in section III for the basis set convergence of each of the energy components, but we shall now apply them to much smaller basis sets to develop a practical scheme. The least expensive MRCI/CBS model chemistry would employ extrapolations from 2ZaP and 3ZaP CAS(10e,8orb)-CISD calculations. It has been noted previously⁵⁶ that DZP basis sets are too small to fit the asymptotic convergence pattern (Figures 7 and 8), but the lower cost of single reference calculations makes it practical to use 3ZaP and 4ZaP calculations to extrapolate to the UHF and CCSD CBS limits, which can then be used to extrapolate the CAS and CAS-CISD energies, respectively.

First, we use an expression analogous to Eq.(5), but applied to the CAS(10e,8orb)/2ZaP and 3ZaP energies to extrapolate to the CAS(10e,8orb)/CBS limit:

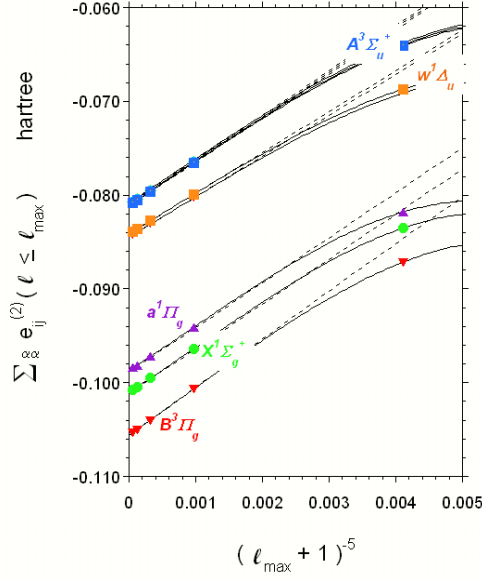


Figure 7. The 2ZaP second-order $\alpha\alpha$ -pair energies do not fit the $(\ell_{\max} + 1)^{-5}$ asymptotic form.

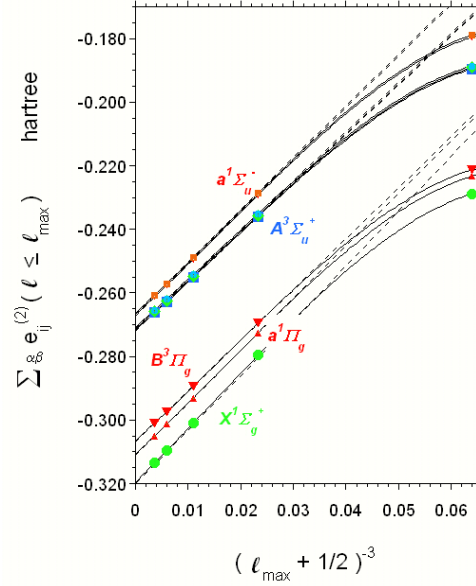


Figure 8. The 2ZaP second-order $\alpha\beta$ -pair energies do not fit the $(\ell_{\max} + 1/2)^{-3}$ asymptotic form.

$$E_{CAS}(CBS) \cong E_{CAS}(3ZaP) + 1.205 [E_{UHF}(4ZaP) - E_{UHF}(3ZaP)] \left[\frac{E_{CAS}(3ZaP) - E_{CAS}(2ZaP)}{E_{UHF}(3ZaP) - E_{UHF}(2ZaP)} \right], \quad (22)$$

where the coefficient, 1.205 is obtained from Eq.(2) with $a=5$.¹⁵ This extrapolation reduces the rms error in the absolute CAS(10,8) energy [relative to the CAS/CBS limit from Eq.(5)] for the eight N_2 states and their dissociation limits from 3.58 mE_h for the CAS(10,8)/3ZaP energies to 0.18 mE_h for the extrapolated values.

The CAS-CISD extrapolation will employ the CCSD/CBS limit, which in turn is obtained from the MP2/CBS limit. The MP2 $\alpha\alpha$ - and $\alpha\beta$ -pair energies must be extrapolated separately using forms analogous to Eq.(7) and Eq.(9) respectively:

$$\sum_{i,j}^{occ} \alpha\alpha e_{ij}^{(2)}(CBS) \cong \sum_{i,j}^{occ} \alpha\alpha e_{ij}^{(2)}(4ZaP) + \frac{(4+1)^{-5}}{(3+1)^{-5} - (4+1)^{-5}} \left\{ \sum_{i,j}^{occ} \alpha\alpha e_{ij}^{(2)}(4ZaP) - \sum_{i,j}^{occ} \alpha\alpha e_{ij}^{(2)}(3ZaP) \right\}, \quad (23)$$

and:

$$\sum_{i,j}^{occ} \alpha\beta e_{ij}^{(2)}(CBS) \cong \sum_{i,j}^{occ} \alpha\beta e_{ij}^{(2)}(4ZaP) + \frac{(4+1/2)^{-3}}{(3+1/2)^{-3} - (4+1/2)^{-3}} \left\{ \sum_{i,j}^{occ} \alpha\beta e_{ij}^{(2)}(4ZaP) - \sum_{i,j}^{occ} \alpha\beta e_{ij}^{(2)}(3ZaP) \right\}. \quad (24)$$

These extrapolations reduce the rms error in the absolute valence MP2 correlation energy (relative to the MP2/CBS limit) for the eight N_2 states and their dissociation limits from 24.53 mE_h for the MP2/4ZaP valence shell correlation energies to 0.99 mE_h for the extrapolated values.

The CBS limit for the CCSD energy includes the interference effect described in section III.D:

$$E_{CCSD}(CBS) \cong E_{CCSD}(4ZaP) + [E_{MP}^{(2)}(CBS) - E_{MP}^{(2)}(4ZaP)] + \Delta E_{CBS-int}(4ZaP, N_{min} = 15), \quad (25)$$

This extrapolation reduces the rms error in the absolute valence CCSD correlation energy [relative to the CCSD/CBS limit from Eq.(18)] for the eight N₂ states and their dissociation limits from 15.84 mE_h for the CCSD/4ZaP valence shell correlation energies to 2.27 mE_h for the extrapolated values.

The CBS limit of the CAS-CISD dynamic correlation energy, $E_{CAS-CISD} - E_{CAS}$, is now estimated from the CCSD CBS limit:

$$\Delta E_{CISD}(CBS) \cong \Delta E_{CISD}(3ZaP) + [\Delta E_{CCSD}(CBS) - \Delta E_{CCSD}(3ZaP)] \left[\frac{\Delta E_{CISD}(3ZaP) - \Delta E_{CISD}(2ZaP)}{\Delta E_{CCSD}(3ZaP) - \Delta E_{CCSD}(2ZaP)} \right], \quad (26)$$

This extrapolation reduces the rms error in the absolute valence CAS(10,8)-CISD dynamic correlation energy (relative to the CAS-CISD/CBS limit from Table VIII) for the eight N₂ states and their dissociation limits from 41.91 mE_h for the CAS-CISD/3ZaP valence shell dynamic correlation energies to 3.18 mE_h for the extrapolated values. Finally, we combine the CAS/CBS energy from Eq.(22) with the $\Delta E_{CISD}/CBS$ energy from Eq.(26) and the PNO extrapolations of the core-core and core valence CCSD(T) correlation energies using the 4ZaPcore basis set:

$$E_{CAS-CISD}(CBS) = E_{CAS}(CBS) + \Delta E_{CISD}(CBS) + \Delta E_{Core}/4ZaPcore. \quad (27)$$

The rms error in the total CAS(10,8)-CISD/CBS energy has been reduced from 45.47 mE_h for the CAS-CISD/3ZaP energies to 3.05 mE_h for the extrapolated values. The extrapolation has *no adjustable parameters*. The results in Table XIX should therefore be typical of the accuracy to be expected in applications. The CAS-CISD/3ZaP anharmonic constants, $\omega_e X_e$, were used in Table XIX without extrapolation, since extrapolated fourth derivatives proved unreliable.

The values obtained for R_e, ω_e , $\omega_e X_e$, T_e and D_e from the CBS extrapolations of CAS-CISD/2ZaP and 3ZaP calculations agree with experiment as well as our best estimates of the CAS-CISD/CBS values obtained from CBS extrapolations of CAS-CISD/4ZaP and 5ZaP calculations. The consistent overestimation of excitation energies in Table XIX is completely consistent with the results in Table XVI. The full valence CAS wave function includes more virtual orbitals and thus more correlation energy for the ground state than for the excited states. The full CI correction (or a model to estimate this correction) to the CAS-CISD energy will be required to improve the accuracy of the excitation energies. This correction necessarily depends on the number of valence

Table XIX. Results obtained from from Eq.(22) through Eq.(27).

State	$R_e(\text{\AA})$	$\omega_e(\text{cm}^{-1})$	$\omega_e X_e(\text{cm}^{-1})$	$T_e(\text{eV})$	$D_e(\text{eV})$
$X^1\Sigma_g^+$	1.0986	2353.24	13.97		9.895
$A^3\Sigma_u^+$	1.2878	1462.58	13.60	6.230	3.671
$B^3\Pi_g$	1.2127	1739.23	13.62	7.469	4.848
$W^3\Delta_u$	1.2802	1505.93	12.01	7.467	4.852
$B'^3\Sigma_u^-$	1.2783	1518.40	11.63	8.275	5.251
$a'^1\Sigma_u^-$	1.2752	1535.06	12.07	8.500	6.216
$a^1\Pi_g$	1.2211	1693.27	13.72	8.646	6.078
$w^1\Delta_u$	1.2683	1565.87	11.60	9.038	5.717
Rms error					
Eq.(22) – Eq.(27)	0.0006	4.43	0.35	0.063	0.018
CAS-CISD/3ZaP	0.0082	18.72	0.35	0.055	0.294

electrons, so a model must be developed with a broader set of examples than the low-lying states of N_2 considered here.

V. CONCLUSIONS

Just as the basis set convergence of the UHF SCF energy provided a model for the basis set convergence of the CASSCF energy, the UCCSD dynamic correlation energy provides a model for the basis set convergence of the CAS-CISD dynamic correlation energy. This can be exploited with extrapolations based on Eq.(22) through Eq.(27), which can reduce basis set truncation errors by more than an order-of-magnitude. However, accurate descriptions of excited state potential energy surfaces also require inclusion of FCI and core electron contributions.

The quality of the results obtained with the relatively modest calculations in Table XIX based on CAS-CISD/3ZaP calculations with the extrapolations in Eq.(22) through Eq.(27) will be quite sufficient for many purposes. This provides a basis for optimism that a practical CBS model chemistry for excited states can be developed. We stress that many more benchmark systems must be examined in order to obtain a reliable and general extrapolation method for multi-reference states. In particular, the effectiveness of extrapolations near electronic state curve crossings, which can have a profound effect on dynamics, will be the subject of future work. In addition, the practicality of performing

the basic CAS-CISD/3ZaP calculations on chemical systems with many atoms must also be addressed.

ACKNOWLEDGMENTS

We acknowledge support through a Small Business Innovative Research (SBIR) award from the Missile Defense Agency (MDA) Contract No. F04611-03-C-0015, and technical oversight from Dr. Marty Venner of the Air Force Research Laboratory. We are also grateful to Gaussian Inc. and Wesleyan University for the support of this research.

REFERENCES

1. R. J. Bartlett and G. D. Purvis, *Int. J. Quant. Chem.* **14**, 516 (1978); G. D. Purvis and R. J. Bartlett, *J. Chem. Phys.* **76**, 1910 (1982).
2. J. A. Pople, M. Head-Gordon, and K. Raghavachari, *J. Chem. Phys.* **87**, 5968 (1987); K. Raghavachari, G. W. Trucks, J. A. Pople, and M. Head-Gordon, *Chem. Phys. Lett.* **157**, 479 (1989).
3. K. Andersson, P. Malmqvist, and B. Roos, *J. Chem. Phys.* **96**, 1218 (1992).
4. B. Huron, P. Rancurel, and J. P. Malrieu, *J. Chem. Phys.* **75**, 5745 (1973).
5. R. J. Buenker and S. D. Peyerimhoff, *Theoret. Chim. Acta* **35**, 33 (1974).
6. B. J. Moss and W. A. Goddard, *J. Chem. Phys.* **63**, 3523 (1975).
7. J. Olsen, B. O. Roos, P. Jørgensen, and H. J. A. Jensen, *J. Chem. Phys.* **89**, 2185 (1988).
8. G. A. Petersson, pp. 237, In *Computational Thermochemistry. ACS Symposium Series 677*, K. K. Irikura and D. J. Frurip, Eds., American Chemical Society, Washington, D. C., 1998.
9. L. A. Curtiss, K. Raghavachari, G. W. Trucks and J. A. Pople, *J. Chem. Phys.* **94**, 7221 (1991).
10. M. R. Zachariah and C. F. Melius, pp. 162, In *Computational Thermochemistry. ACS Symposium Series 677*, K. K. Irikura and D. J. Frurip, Eds., American Chemical Society, Washington, D. C., 1998.
11. M. R. Nyden and G. A. Petersson, *J. Chem. Phys.* **75**, 1843 (1981).
12. G. A. Petersson, pp. 99, In *Quantum-Mechanical Prediction of Thermochemical Data*, J. Cioslowski, Ed., Kluwer Academic Publishers, Dordrecht, the Netherlands, 2001.
13. T. H. Dunning, Jr., *J. Chem. Phys.* **90**, 1007 (1989).
14. J. M. L. Martin, pp. 212, In *Computational Thermochemistry. ACS Symposium Series 677*, K. K. Irikura and D. J. Frurip, Eds., American Chemical Society, Washington, D. C., 1998.
15. G. A. Petersson, D. K. Malick, M. J. Frisch, and M. Braunstein, *J. Chem. Phys.* **123**, 74111 (2005).
16. T. Xie, J. Bowman, M. Braunstein, J. Duff, and B. Ramachandran, *J. Chem. Phys.* **122**, 014301 (2005).
17. L. Bernstein, Y. Chiu, J. A. Gardner, A. L. Broadfoot, M. Lester, M. Tsiouris, R. Dressler, and E. Murad, *J. Phys. Chem.* **107**, 10695 (2003).
18. O. J. Orient, A. Chutijan, and E. Murad, *Phys. Rev. Lett.* **65**, 2359 (1990).
19. S. Matsika and D. R. Yarkony, *J. Chem. Phys.* **117**, 3733 (2002).
20. D.J. Garton, T.K. Minton, D. Troya, R. Pascual, and G.C. Schatz, *J. Phys. Chem. A* **107**, 4583-4587 (2003).
21. G. A. Petersson, S. Zhong, J. A. Montgomery, Jr., and M. J. Frisch, *J. Chem. Phys.* **118**, 1101 (2003).
22. S. Zhong, D. Ashen-Garry, and G. A. Petersson, "The nZaP Basis Sets, I. Uniformly Convergent Basis Sets for CBS Extrapolations of SCF Energies", in preparation.
23. Ericka Barnes, Frank Dobeck, and G. A. Petersson, manuscript in preparation.
24. D. Hegarty and M. A. Robb, *Mol. Phys.* **38**, 1795 (1979).
25. R. H. E. Eade and M. A. Robb, *Chem. Phys. Lett.* **83**, 362 (1981).
26. B. O. Roos, P. Linse, P. E. M. Siegbahn, and M. R. A. Blomberg, *Chem. Phys.* **66**, 197 (1981).
27. H. B. Schlegel and M. A. Robb, *Chem. Phys. Lett.* **93**, 43 (1982).
28. M. J. Frisch, I. N. Ragazos, M. A. Robb, and H. B. Schlegel, *Chem. Phys. Lett.* **189**, 524 (1992).
29. J. A. Pople, in *Energy, Structure and Reactivity*, edited by D. W. Smith and W. B. McRae (Wiley, New York, 1973), p. 51.
30. J. A. Pople, J. S. Binkley, and R. Seeger, *Int. J. Quantum Chem. Symp.* **10**, 1 (1976).
31. R. Krishnan and J. A. Pople, *Int. J. Quantum Chem.* **14**, 91 (1978).
32. K.P. Huber and G. Herzberg, "Constants of Diatomic Molecules" (data prepared by J.W. Gallagher and R.D. Johnson, III) in **NIST Chemistry WebBook, NIST Standard Reference Database Number 69**,

- Eds. P.J. Linstrom and W.G. Mallard, June 2005, National Institute of Standards and Technology, Gaithersburg MD, 20899 (<http://webbook.nist.gov>).
33. Gaussian 03, Revision B.04, M. J. Frisch, G. W. Trucks, *et al.*, Gaussian, Inc., Wallingford CT, 2004.
 34. H. Lischka, R. Shepard, F. B. Brown and I. Shavitt, *Int. J. Quantum Chem., Quantum Chem. Symp.*, 1981, **15**, 91.
 35. R. Shepard, I. Shavitt, R. M. Pitzer, D. C. Comeau, M. Pepper, H. Lischka, P. G. Szalay, R. Ahlrichs, F. B. Brown, and J. Zhao *Int. J. Quantum Chem., Quantum Chem. Symp.*, 1988, **22**, 149.
 36. H. Lischka, R. Shepard, R. M. Pitzer, I. Shavitt, M. Dallos, Th. Müller, P. G. Szalay, M. Seth, G. S. Kedziora, S. Yabushita and Z. Zhang *Phys. Chem. Chem. Phys.*, 2001, **3**, 664.
 37. H. Lischka, R. Shepard, I. Shavitt, *et al.*, COLUMBUS, an *ab initio* electronic structure program, release 5.9.6 (2003).
 38. F. B. van Duijneveldt, IBM Publ. RI 945, Yorktown Hts., New York, 1971.
 39. W. Klopper and W. Kutzelnigg, *J. Mol. Struct.* **135**, 339 (1986).
 40. W. Kutzelnigg pp79-101 in: *Strategies and applications in quantum chemistry*, Y. Ellingr and M. Defranceschi Eds., Kluwer, Dordrecht, the Netherlands , 1996.
 41. F. Jensen, *Theor. Chem. Acc.* **113**, 187 (2005).
 42. C. Schwartz, *Phys. Rev.* **126**, 1015 (1962).
 43. C. Schwartz, in *Methods in Computational Physics*, edited by B. Alder, S. Fernbach, and M. Rotenberg (Academic Press. New York, 1963), Vol. 2, pp. 262-265.
 44. C. F. Bunge, *Phys. Rev. A* **14**, 1965 (1976).
 45. K. Jankowski and P. Malinowski, *Phys. Rev. A* **21**, 45 (1980).
 46. J. W. Ochterski, G. A. Petersson, and J. A. Montgomery, Jr., *J. Chem. Phys.* **104**, 2598 (1996).
 47. G. A. Petersson and M. R. Nyden, *J. Chem. Phys.* **75**, 3423 (1981).
 48. G. A. Petersson and S. L. Licht, *J. Chem. Phys.* **75**, 4556 (1981).
 49. G. A. Petersson and M. J. Frisch, *J. Phys. Chem. A* **104**, 2183 (2000).
 50. L. Bytautas and K. Ruedenberg, *J. Chem. Phys.* **122**, 154110 (2005).
 51. H. Larsen, J. Olsen, and P. Jørgensen, *J. Chem. Phys.* **113**, 6677 (2000).
 52. G. A. Petersson, A. Bennett, T. G. Tensfeldt, M. A. Al-Laham, W. A. Shirley, and J. Mantzaris, *J. Chem. Phys.* **89**, 2193 (1988).
 53. J. Noga, P. Valiron, and W. Klopper, *J. Chem. Phys.* **115**, 2022 (2001).
 54. X. Tang, Y. Hou, C. Y. Ng, and B. Ruscic, *J. Chem. Phys.* **123**, 74330 (2005).
 55. W. C. Martin, J. Sugar, and A. Musgrove, *NIST Atomic Spectra Database, NIST Standard Reference Database #78* (2005).
 56. G. A. Petersson and M. J. Frisch, *J. Phys. Chem.* **104**, 2183 (2000).